

## Gap anisotropy and phonon self-energy effects in single-crystal $\text{YBa}_2\text{Cu}_3\text{O}_{7-\delta}$

S. L. Cooper,\* F. Slakey, M. V. Klein, J. P. Rice, E. D. Bukowski, and D. M. Ginsberg  
*Department of Physics and Materials Research Laboratory, University of Illinois at Urbana-Champaign,  
 1110 W. Green St., Urbana, Illinois 61801*  
 (Received 8 September 1988)

We report a Raman scattering investigation of superconducting gap anisotropy in single-crystal  $\text{YBa}_2\text{Cu}_3\text{O}_{7-\delta}$ . Gap anisotropy is investigated by studying the peak in the low-temperature Raman continuum in various symmetries. Roughly a 35% difference in the energy of this peak is observed between different symmetries, suggesting the presence of substantial gap anisotropy. Anisotropy is further evidenced by the damping behavior of the  $340\text{-cm}^{-1}$  Raman-active phonon below  $T_c$ , which displays increased attenuation due to phonon-induced pair breaking. The temperature dependence of this attenuation is consistent with a  $T=0$  pair-breaking peak which is much larger than the  $340\text{-cm}^{-1}$  phonon in certain regions of the Fermi surface.

Many of the recent experimental studies of  $\text{YBa}_2\text{Cu}_3\text{O}_{7-\delta}$  have been devoted to understanding the nature of the superconducting gap in this compound. Unfortunately, even an identification of the pairing strength in  $\text{YBa}_2\text{Cu}_3\text{O}_{7-\delta}$  has been obscured by the diversity of gap parameters ( $r=2\Delta/k_B T_c$ ) reported for this material. For example, while infrared reflectivity measurements<sup>1-3</sup> have generally afforded gap parameters which are consistent with weak-coupling Bardeen-Cooper-Schrieffer (BCS) theory ( $r\sim 3.5$ ), tunneling measurements<sup>4-6</sup> exhibit gap parameters which are well within the strong-coupling regime ( $r\sim 4.8$ ). More recently, a theoretical analysis of the softening of certain Raman-active<sup>7-9</sup> and infrared-active<sup>10</sup> phonons below  $T_c$  has concluded that  $\text{YBa}_2\text{Cu}_3\text{O}_{7-\delta}$  is in the strong-coupling limit.<sup>11</sup> This conclusion is based on the assumption that the renormalized phonons have energies larger than the superconducting gap,  $\hbar\omega > 2\Delta$  ( $T=0$ ).

In this paper, we present a Raman scattering study of the superconducting gap in single-crystal  $\text{YBa}_2\text{Cu}_3\text{O}_{7-\delta}$ , in an attempt to understand the conflicting results listed above. The efficacy of using this technique to probe the superconducting gap has been demonstrated in polycrystalline<sup>12,13</sup> and single-crystal<sup>9</sup> samples of  $\text{YBa}_2\text{Cu}_3\text{O}_{7-\delta}$ . The present Raman scattering investigation extends these results to the study of the symmetry properties of  $2\Delta$ . Our data provide evidence for substantial gap anisotropy in  $\text{YBa}_2\text{Cu}_3\text{O}_{7-\delta}$ , and thus may afford insight into the structure of the superconducting gap. Furthermore, in addition to the phonon frequency renormalization which has been observed earlier below  $T_c$ ,<sup>7-10</sup> we present new evidence that superconductivity dramatically affects the lifetime of one of the observed Raman-active phonons. The damping behavior of this phonon below  $T_c$  is consistent with possible gap anisotropy in  $\text{YBa}_2\text{Cu}_3\text{O}_{7-\delta}$ .

The  $\text{YBa}_2\text{Cu}_3\text{O}_{7-\delta}$  samples used in this study were pure-phase single crystals having narrow transition temperatures near  $T_c=90$  K. The preparation of these samples has been described elsewhere.<sup>9</sup> Raman scattering measurements on  $\text{YBa}_2\text{Cu}_3\text{O}_{7-\delta}$  single crystals were performed in a near backscattering geometry, with light polarized in the  $a$ - $b$  plane. A number of scattering geometries

were studied in this investigation, including polarized  $(y,y)$  and  $(y',y')$  [ $y=(0,1,0)$ ;  $y'=(1/\sqrt{2})(1,1,0)$ ] geometries and depolarized  $(y,x)$  and  $(y',x')$  [ $x=(1,0,0)$ ;  $x'=(1/\sqrt{2})(-1,1,0)$ ] geometries. Considered within the tetragonal point group, these geometries allow coupling to  $A_{1g}+B_{1g}$ ,  $A_{1g}$ ,  $B_{2g}$ , and  $B_{1g}$  symmetries, respectively.

Figure 1 illustrates the 300-K Raman scattering spectra of single-crystal  $\text{YBa}_2\text{Cu}_3\text{O}_{7-\delta}$  in a number of scattering geometries. Each dashed line shown in Fig. 1 defines the zero intensity level for the spectrum directly above it. The

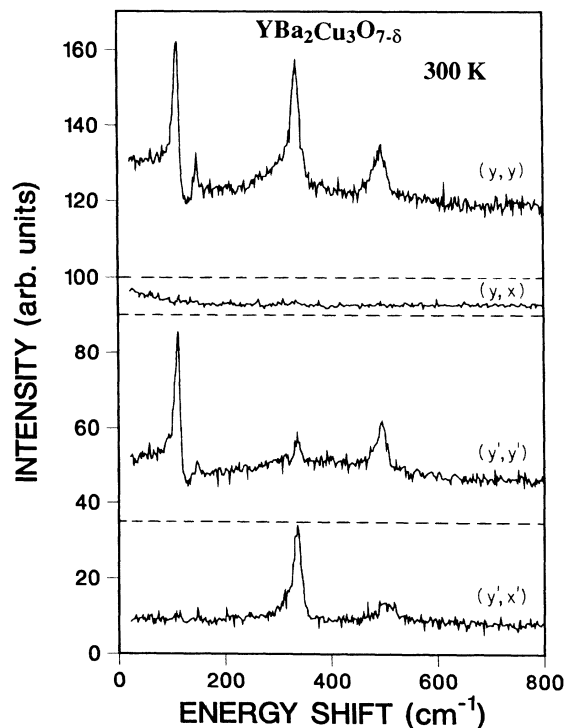


FIG. 1. 300-K spectra of single-crystal  $\text{YBa}_2\text{Cu}_3\text{O}_{7-\delta}$  for various scattering geometries, including  $(y,y)$  [ $A_{1g}+B_{1g}$  (tetragonal)],  $(y,x)$  ( $B_{2g}$ ),  $(y',y')$  ( $A_{1g}$ ), and  $(y',x')$  ( $B_{1g}$ ). Each dashed line indicates the zero-intensity level for the spectrum immediately above it. Resolution:  $4\text{ cm}^{-1}$ .

top,  $(y,y)$  ( $A_{1g} + B_{1g}$ ), spectrum demonstrates a number of optical phonon peaks, as well as an intense electronic background which strongly interferes with the optical phonons at 116 and 340  $\text{cm}^{-1}$ .<sup>9</sup> These interference effects are reflected in the asymmetric line shapes associated with the 116 and 340  $\text{cm}^{-1}$  phonons, as well as in the "antiresonance" evident on the high-energy side of the 116- $\text{cm}^{-1}$  mode. The 340- $\text{cm}^{-1}$  phonon is particularly notable in that it switches to the *depolarized*  $(y',x')$  spectrum upon rotating the incidence polarization by 45° [see  $(y',y')$  and  $(y',x')$  in Fig. 1]. This suggests that, within the tetragonal point group, the 340- $\text{cm}^{-1}$  phonon transforms according to the  $B_{1g}$  representation, while all of the other Raman-active phonons have  $A_{1g}$  symmetry.<sup>14</sup>

Figure 1 also illustrates that the electronic continuum background has both  $A_{1g}$  [ $(y',y')$ ] and  $B_{1g}$  [ $(y',x')$ ] contributions, as may be observed by comparing the background levels of the four spectra shown in Fig. 1. Indeed, the interference effects associated with the 116  $\text{cm}^{-1}$   $A_{1g}$  and 340  $\text{cm}^{-1}$   $B_{1g}$  phonons confirm that the electronic continuum has both  $A_{1g}$  and  $B_{1g}$  symmetries, since phonons only interfere with a continuum of like symmetry. Note also that the  $B_{2g}$  [ $(y,x)$ ] spectrum manifests a negligible electronic continuum contribution, while the  $A_{1g} + B_{1g}$  [ $(y,y)$ ] background is simply the sum of the  $(y',y')$  and  $(y',x')$  contributions.

Figure 2 shows the  $(y',y')$  ( $A_{1g}$ ) and  $(y',x')$  ( $B_{1g}$ ) spectra well below  $T_c$ , allowing us to separately examine the effects of the superconducting gap on the  $A_{1g}$  and  $B_{1g}$  contributions to the electronic continuum. The electronic continuum in both these symmetries displays a loss of scattering strength at low energies, as electronic scattering

below  $2\Delta$  is suppressed by the opening gap. As reported earlier,<sup>9</sup> this suppression is incomplete, as evidenced by the residual low-energy electronic scattering present in both spectra of Fig. 2. Furthermore, a peak in the continuum, which is believed to arise from the direct excitation of superconducting quasiparticles above the gap ( $2\Delta$ ), is apparent in both symmetries. It is evident in Fig. 2 that the pair-breaking peak in the  $B_{1g}$  spectrum occurs at roughly a 35% larger energy than is observed in the  $A_{1g}$  spectrum. Specifically, the  $A_{1g}$  continuum is observed to peak near the 340- $\text{cm}^{-1}$   $B_{1g}$  phonon, while the  $B_{1g}$  continuum peaks well above the  $B_{1g}$  phonon, at roughly 530  $\text{cm}^{-1}$ . Additionally, in the 15-K  $B_{1g}$  spectrum, the suppression of the continuum intensity below its normal-state value is evident at much higher frequencies than is observed in the 15-K  $A_{1g}$  spectrum. Note that the  $(y,y)$  ( $A_{1g} + B_{1g}$ ) spectrum is simply the sum of the  $(y',y')$  and  $(y',x')$  contributions, and, therefore, does not provide independent symmetry information. Furthermore, due to the absence of an electronic continuum in the  $(y,x)$  spectrum, no gap structure is observed in this symmetry.

The disparity between the  $A_{1g}$  and  $B_{1g}$  low-temperature spectra appears to reveal substantial gap anisotropy in  $\text{YBa}_2\text{Cu}_3\text{O}_{7-\delta}$ . A precise estimate of this anisotropy is difficult, due to the absence of a well-defined gap in these spectra.<sup>9</sup> However, it appears that the pair-breaking energy associated with  $B_{1g}$  symmetry is roughly 35% larger than that having  $A_{1g}$  symmetry. In order to isolate the origin of this anisotropy, we note that light scatters from superconducting gap excitations through fluctuations in the matrix element,  $\gamma_{\mathbf{k}}$ , where  $\gamma_{\mathbf{k}}$  is related to the inverse effective-mass tensor,  $\mu_{\mathbf{k}}^{-1}$ . Because deviations of the  $\text{YBa}_2\text{Cu}_3\text{O}_{7-\delta}$  structure from  $D_{4h}$  symmetry are small, we may decompose this matrix element into irreducible tensor components of the tetragonal space group. Those tensor components relevant to our data are given by

$$|\gamma^{A_{1g}}|^2 = \frac{1}{3} |\text{Tr} \gamma|^2, \quad (1)$$

$$|\gamma^{B_{1g}}|^2 = |\gamma^{xx} - \gamma^{yy}|^2. \quad (2)$$

Equations (1) and (2) illustrate that whereas the  $A_{1g}$  Raman contribution to the gap represents an average gap value, the  $B_{1g}$  spectra should arise from those regions of the Fermi surface in which the inverse effective masses in the  $x$  and  $y$  directions have the largest differences. Our results consequently suggest that the gap associated with Fermi-surface regions in which  $|(\mu^{-1})^{xx} - (\mu^{-1})^{yy}|^2$  is large should be roughly 35% larger than the average ( $A_{1g}$ ) gap. Detailed Fermi-surface calculations are needed to elucidate the shape of the Fermi surface in  $\text{YBa}_2\text{Cu}_3\text{O}_{7-\delta}$ . However, because the Fermi surface associated with the Cu-O chains should manifest extremely large effective-mass differences between the  $x$  and  $y$  directions, it is tempting to speculate that the large gap apparent in the  $B_{1g}$  Raman spectrum is related to the Cu-O chains.

The high energy of the  $B_{1g}$  pair-breaking peak also appears to be reflected by phonon renormalization effects in the superconducting phase. This is demonstrated in Fig. 3, where we show the phonon spectra of the Fano-coupled

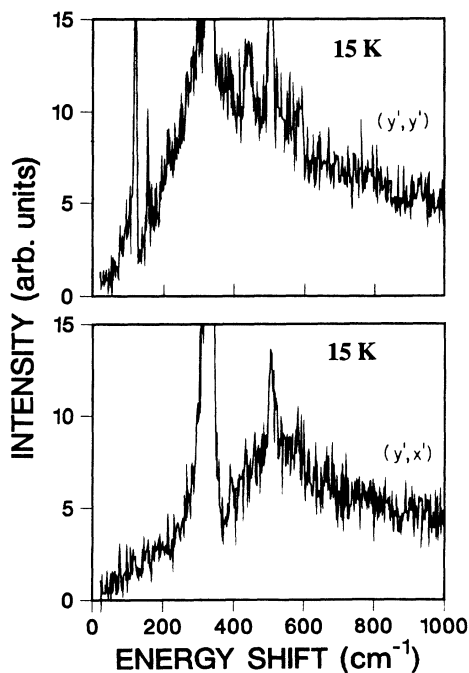


FIG. 2. Polarized [ $(y',y') = A_{1g}$ ] spectrum (top) and depolarized [ $(y',x') = B_{1g}$ ] spectrum (bottom) well below  $T_c$  (15 K) in single-crystal  $\text{YBa}_2\text{Cu}_3\text{O}_{7-\delta}$ , illustrating the large difference in gap structures in these two symmetries. Resolution: 4  $\text{cm}^{-1}$ .

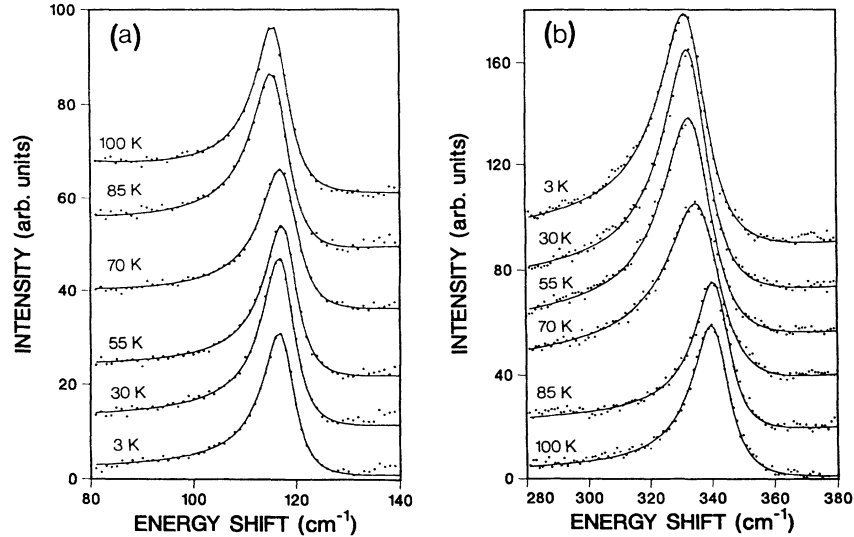


FIG. 3. Temperature dependence of the (a)  $A_{1g}$  phonon at  $116\text{ cm}^{-1}$  and the (b)  $B_{1g}$  phonon at  $340\text{ cm}^{-1}$  below  $T_c$ . These phonons have been fit to a Fano line shape (solid lines) as described in the text. Note that the temperature increases from bottom to top in (a) and from top to bottom in (b).

$116\text{-cm}^{-1}$   $A_{1g}$  (tetragonal) and  $340\text{-cm}^{-1}$   $B_{1g}$  (tetragonal) phonons below  $T_c$ . The coupling of these two phonons to the electronic continuum is illustrated by fits to a Fano line shape in Fig. 3 (solid line)

$$S(\omega) \propto \frac{[1 - \exp(\hbar\omega/k_B T)]^{-1} 2\Gamma\omega(\Omega_a^2 - \omega^2)^2}{(\omega_0^2 - \omega^2)^2 + 4\Gamma^2\omega^2}, \quad (3)$$

where  $\Omega_a$  is the antiresonance frequency,  $\Gamma$  is the coupled-phonon linewidth, and  $\omega_0$  is the renormalized phonon frequency. In addition to displaying a Fano line shape, the  $340\text{-cm}^{-1}$  phonon manifests an abrupt softening below  $T_c$  (between 85-K and 70-K spectra in Fig. 3). This softening has been attributed to phonon self-energy effects, wherein the phonon frequency is screened by the superconducting quasiparticles.<sup>11,14</sup> Additionally, our phonon results indicate an abrupt enhancement in the damping of the  $340\text{-cm}^{-1}$  phonon just below  $T_c$  (see Fig. 3), which is followed by a decreased damping at still lower temperatures. The behavior of the  $340\text{-cm}^{-1}$  phonon linewidth  $\Gamma$  below  $T_c$  is illustrated in Fig. 4. These phonon renormalization effects (see Figs. 3 and 4) are much more striking than those observed previously,<sup>9</sup> due to the sharper transition temperatures of the present samples. We attribute the increased phonon damping in the superconducting phase to the presence of a phonon-induced pair-breaking relaxational channel which is allowed for phonons satisfying  $\hbar\omega > 2\Delta(T)$ . Note particularly that the sharp enhancement, then gradual decrease of the  $340\text{-cm}^{-1}$  linewidth below  $T_c$  suggests that the “center of mass” of the  $B_{1g}$  pair-breaking energy distribution moves through the  $B_{1g}$  phonon frequency as a function of temperature.<sup>15</sup> The fact that the  $B_{1g}$  phonon attenuation does not drop discontinuously, or even significantly, as in the case of a superconductor with a well-defined gap,<sup>15</sup> is presumably due to the absence of a distinct gap in  $\text{YBa}_2\text{Cu}_3\text{O}_{7-\delta}$  (see Fig. 2 and Ref. 9). Thus, the temper-

ature dependence of the  $B_{1g}$  phonon linewidth below  $T_c$  is further confirmation that the  $B_{1g}$  pair-breaking energy at  $T=0$  peaks at a significantly higher energy than that of the  $340\text{-cm}^{-1}$  phonon.

In conclusion, we have presented strong Raman evidence for substantial superconducting gap anisotropy in single crystal  $\text{YBa}_2\text{Cu}_3\text{O}_{7-\delta}$ . Specifically, the quasiparticle pair-breaking peak in the  $B_{1g}$  Raman spectrum appears to occur at a significantly higher energy ( $\sim 530\text{ cm}^{-1}$ ) than that found in the  $A_{1g}$  spectrum ( $\sim 340\text{ cm}^{-1}$ ). Additionally, in the  $B_{1g}$  spectrum suppression of the low-frequency continuum occurs to much higher energies than in the  $A_{1g}$  spectrum. These results suggest that the largest gaps are associated with those regions of the Fermi surface which exhibit large reciprocal effective-mass differences between the  $x$  and  $y$  directions. These re-

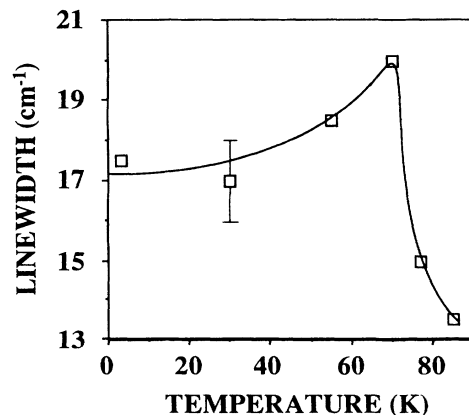


FIG. 4. Observed temperature dependence of the  $340\text{ cm}^{-1}$  phonon linewidth  $\Gamma$  below  $T_c$  (open squares), illustrating the dramatic damping enhancement below the superconducting transition. The solid line is a guide to the eye.

sults also suggest that the diversity of gap energies observed by different techniques may simply reflect the large gap anisotropy apparent in  $\text{YBa}_2\text{Cu}_3\text{O}_{7-\delta}$ . Finally, we have also observed phonon self-energy effects below  $T_c$  related to the damping behavior of the  $340\text{-cm}^{-1}$  Raman-active phonon. This phonon exhibits an abrupt linewidth increase below  $T_c$  which is thought to arise from phonon-induced quasiparticle pair breaking. The behavior of this phonon linewidth with temperature below  $T_c$  is also con-

sistent with an average  $B_{1g}$  pair-breaking energy (at  $T=0$ ) which is significantly larger than the  $340\text{-cm}^{-1}$  phonon frequency.

The Raman scattering work was supported by the National Science Foundation under Grant No. DMR 87-15103, and the single-crystal treatment and growth were supported by National Science Foundation Grant No. DMR 87-14555.

\*Present address: AT&T Bell Laboratories, 600 Mountain Ave., Murray Hill, NJ 07974.

<sup>1</sup>J. R. Kirtley, R. T. Collins, Z. Schlesinger, W. J. Gallagher, R. L. Sandstrom, T. R. Dinger, and D. A. Chance, *Phys. Rev. B* **35**, 8846 (1987).

<sup>2</sup>D. A. Bonn, J. E. Greedan, C. V. Stager, T. Timusk, M. G. Doss, S. L. Herr, K. Kamaras, and D. B. Tanner, *Phys. Rev. Lett.* **58**, 2249 (1987).

<sup>3</sup>G. A. Thomas, H. K. Ng, A. J. Millis, R. N. Bhatt, R. J. Cava, E. A. Rietman, D. W. Johnson, Jr., G. P. Espinosa, and J. M. Vandenberg, *Phys. Rev. B* **36**, 846 (1987).

<sup>4</sup>J. Moreland, J. W. Ekin, L. F. Goodrich, T. E. Capobianco, A. F. Clark, J. Kwo, M. Hong, and S. H. Liou, *Phys. Rev. B* **35**, 8856 (1987).

<sup>5</sup>I. Iguchi, H. Watanabe, Y. Kasai, T. Mochiku, A. Sugishita, and E. Yamaka, *Jpn. J. Appl. Phys.* **26**, L645 (1987).

<sup>6</sup>J. R. Kirtley, C. C. Tsuei, S. I. Park, C. C. Chi, J. Rozen, and M. W. Shafer, *Phys. Rev. B* **35**, 7216 (1987).

<sup>7</sup>R. M. Macfarlane, H. Rosen, and H. Seki, *Solid State Commun.* **63**, 831 (1988).

<sup>8</sup>A. Wittlin, R. Liu, M. Cardona, L. Genzel, W. König, M. V.

Cabanas, and E. Garcia-Alvarado, *Solid State Commun.* **64**, 477 (1987).

<sup>9</sup>S. L. Cooper, M. V. Klein, B. G. Pazol, J. P. Rice, and D. M. Ginsberg, *Phys. Rev. B* **37**, 5920 (1988).

<sup>10</sup>C. Thomsen, R. Liu, A. Wittlin, L. Genzel, M. Cardona, W. König, M. V. Cabanas, and E. Garcia, *Solid State Commun.* **65**, 219 (1988).

<sup>11</sup>R. Zeyher and G. Zwicknagl, *Solid State Commun.* **66**, 617 (1988).

<sup>12</sup>A. V. Bazhenov, A. V. Gorbunov, M. V. Klassen, S. F. Kodakov, I. V. Kukushkin, V. D. Kalakovskii, O. V. Misochko, V. B. Timofeev, L. I. Chernyshova, and B. N. Shepel, in *Novel Superconductivity*, edited by S. A. Wolf and V. Z. Kresin (Plenum, New York, 1987), p. 699; and *Pis'ma Zh. Eksp. Teor. Fiz.* **46**, 35 (1987) [*JETP Lett.* **46**, 32 (1987)].

<sup>13</sup>K. B. Lyons, S. H. Liou, M. Hong, H. S. Chen, J. Kwo, and T. J. Negran, *Phys. Rev. B* **36**, 5592 (1987).

<sup>14</sup>C. Thomsen, M. Cardona, B. Gegenheimer, R. Liu, and R. Simon, *Phys. Rev. B* **37**, 9860 (1988).

<sup>15</sup>V. M. Bobetic, *Phys. Rev.* **136**, A1535 (1964).